Asian Journal of Chemistry Vol. 21, No. 1 (2009), 279-286

Purification of Recombinent p19^{ARF}: Protein Interaction and Stability Analysis

XIN LIU, LIN FANG DU*†‡, XIN HE HUANG, DE YAN ZHU, JIA LI and JING ZHANG WANG
Key Laboratory of Bio-resources and Eco-environment of the Ministry of Education
College of Life Sciences, Sichuan University, 610064 Chengdu, P.R. China
Fax: (86)(28)85415300; Tel: (86)(28)85415008
E-mail: dulinfang@scu.edu.cn

The protein alternate reading frame (ARF) known as p19^{ARF} in mice is unique in its capacity to facilitate cancer suppression. Here, we report that recombinent 10His-p19^{ARF} expressed in *Escherichia coli* BL21 (DE3) could be purified under native condition by nickel chelating affinity chromatography and have functional structure. 0.3 mg 10His-p19^{ARF} per liter culture could be obtained after the purification process. This recombinant protein was recognized by western blot with anti-His antibody. Then GST pull-down assay revealed its interaction with TAp63γ (a member of the p53 family) *in vitro*. By describing its temperature and pH dependent stabilities using fluorescence measurements, the surface environment of the C-terminal region of 10His-p19^{ARF} was especially found to be hydrophobic. The 10His-p19^{ARF} unfolding with heat was a two-state mechanism. A significant change of tryptophan fluorescence of p19^{ARF} upon β-mercaptoethanol suggested its disulfide bond-dependent conformation.

Key Words: Fluorescence spectroscopy, Immobilized metal affinity chromatography, Immunoblot detection, p19^{ARF}, Protein-protein interaction.

INTRODUCTION

The ARF tumour suppressor protein (known as p19^{ARF} in mice and p14^{ARF} in human) is encoded by Ink4a^{ARF} locus, through the use of an alternative reading frame[1,2]. As a tumour suppressor, ARF induces potent growth arrest or cell death in response to hyperproliferative oncogenic stimuli.

†Institute of Nanobiomedical Technology and Membrane Biology, Sichuan University, Chengdu, P.R. China.
‡State Key Laboratory of Biotherapy of Human Diseases, Cancer Center, West China Hospital, West China Medical School, Sichuan University, Chengdu, P.R. China.

ARF can activate the p53 tumor surveillance pathway by directly binding to the p53 negative regulators[3-5]. On the other hand, ARF have p53-independent activities, such as regulating ribosome biogenesis[3,6] and inducing sumoylation or degradation of some cellular proteins[7,8]. Consistent with these significant functions, ARF inactivation is common in many cancers[9-11]. Conversely, medical research on the potential contribution of ARF to growth control *in vivo* and *in vitro* suggested its potential important role in cancer treatment[12-14].

As such an important protein, however, little is known about the molecular properties of ARF. Until now the purification of full length of active ARF has not been reported. Considering the fact that protein purification is an essential step of protein studies, we expressed 10His-$p19^{ARF}$ from *E. coli* and purified the protein using a nicked metal-affinity resin column under native condition. After removing imidazole from the elution sample by dialysis, the product was detected by western blot and accumulated for further research.

p63 is a member of p53 tumour suppressor family. TAp63γ, among the six isotypes of p63, shares the highest sequence and structural homology with p53. By the mouse models, TAp63γ plays not only a key role in tumour suppression but also in development and differentiation[15-17]. On the other hand, in addition to the tumour suppression role, $p19^{ARF}$ also appears to affect mammalian aging[18]. Therefore, the interaction experiment between 10His-$p19^{ARF}$ and TAp63γ was designed in order to suggest that p19ARF might play the different regulating roles through the complex network of p53-like proteins.

In view of the major role of ARF, the functional differences between $p19^{ARF}$ and $p14^{ARF}$ may contribute to the different levels of tumor proneness of the species[19,20]. One basic reason of these functional differences is that $p19^{ARF}$ and $p14^{ARF}$ are substantially divergent at their carboxyl terminal[21]. There were three Trp residues in $p19^{ARF}$ at positions 147, 154 and 161 and two Tyr residues at positions 90 and 159. Since all three Trp residues in $p19^{ARF}$ are just located in its C-terminal region which is missing in $p14^{ARF}$, we tested fluorescence spectra of $p19^{ARF}$ under different physico-chemical conditions to learn structural characters of $p19^{ARF}$, especially the characters of the C-terminal region.

EXPERIMENTAL

A Quick-Clone cDNA library as a template for PCR was purchased from Clontech. Plasmid vector pET19b and *E. coli* strain BL21 (DE3) cells were obtained from Novagen. The Ni-chelating Sepharose and the column were from Amsherm. Anti-His antibody was from Tiangen Biotech. All other reagents were of Analysis Grade and were commercially available.

Expression and purification of p19^{ARF}: The p19^{ARF} was amplified by PCR based on the Quick-Clone cDNA library. The amplified fragment was inserted into pET-19b between BamH I and Nde I sites. The competent cells were prepared by $CaCl_2$ method. *E. coli* BL21 (DE3) harbouring pET^{19b}-p19^{ARF} was cultured at 37 °C in 1 L of Luria-Bertani (LB) broth containing ampicillin (100 μg/mL) until the optical density at 600 nm (OD600) reached 0.6. Protein expression was then induced by incubation adding 1.0 mM isopropyl-β-D-thiogalactopyranoside (IPTG) for 4 h at 37 °C and the cells were harvested by centrifugation at 2200 g for 10 min at 4 °C. The pellets were washed with 100 mL of 50 mM PBS (pH 7.2), resuspended in 40 mL of buffer A (0.5 M NaCl, 50 mM NaH_2PO_4-NaOH, pH 8.0) containing 1 % Tween-20, 0.2 mM β-mercaptoethanol and 50 mM imidazole, then lysed by an ultrasonic oscillator. By centrifugation (13,000 g, 20 min, 4 °C), the cell debris was removed and the resulting supernatant was stored at 4 °C for further purification.

The supernatant of cell lysate was loaded onto a 2 mL Ni-chelating affinity column pre-equilibrated with buffer A in the presence of 50 mM imidazole and mixed with the beads gently by overshaking for 0.5 h. The column was then washed with 40 mL of buffer A containing 100 mM imidazole and sequentially washed with 40 mL of buffer A containing 180 mM imidazole, at a rate of 0.5 mL/min. The His-tag fusion protein was eluted in buffer A with 600 mM imidazole. Imidazole in the elution was removed by dialysis against 50 mM PBS, pH 8.0. The entire process was performed at 4 °C. The protein sample of every step was saved and analyzed by 12 % sodium dodecyl sulfate polyacrylamide gel electrophoresis (SDS-PAGE). The protein bands were visualized by Coomassie brilliant blue R250 staining.

Western blot analysis: For western blot recognition, the purified sample was subjected to 12 % SDS-PAGE controlled by the molecular-mass marker protein. Then the marker protein part of gel was cut for Coomassie brilliant blue R250 staining, while the part of purified sample were transferred to nitrocellulose membranes and developed with the anti-6His antibody and horseradish peroxidase-conjugated secondary antibodies. Horseradish peroxidase activity was detected by ECL.

GST-fusion protein pull-down assay: GST and GST-TAp63γ fusion protein were expressed in and purified from *E. coli* BL21 (DE3). The GST-TAp63γ was immobilized on glutathione-Sepharose beads as the bait for protein interaction. The primal beads and the beads binding with GST protein were prepared as two negative controls. The p19^{ARF} was incubated with beads in buffer C (50 mM PB, pH 8.0, 300 mM NaCl, 1 mM PMSF, 0.1 % (v/v) Triton-X-100) for 4 h at 4 °C. The beads were then washed three times with buffer C and the bound proteins were analyzed by SDS-PAGE[22].

Fluorescence measurements: The intrinsic fluorescence emission measurement of 10His-p19^{ARF} was carried out at 25 °C. 280 nm of excitation wavelength was used to excite the Trp and Tyr side-chains and 295 nm was used to excite the Trp residues only[23]. The stabilities of 10His-p19^{ARF} under different temperature, pH and β-mercaptoethanol concentrations were also investigated by using the intrinsic fluorescence signal.

RESULTS AND DISCUSSION

Expression and purification of 10His-p19^{ARF}: The recombinant plasmid pET19b-p19Arf was sequenced and the homology of the nucleotide sequence was searched by BLAST program through NCBI. The inserted fragment was confirmed to be p19Arf gene (under Accession No. NM 009877).

The supernatant of *E. coli* BL21 (DE3) lysate was subjected to Ni-chelating affinity chromatography and *ca.* 0.3 mg product per liter culture was obtained by testing with Bradford method. As detected by SDS-PAGE, the molecular mass of the product (Fig. 1, lane 4) was *ca.* 22 kDa which agreed well with the calculated mass for 10His-p19^{ARF}. Actually we also experimented to accumulate p14^{ARF} through the similar way, but different from 10His-p19^{ARF}, the recombinant p14^{ARF} mainly expressed as inclusion body and was difficult to be refolded for the following function assay, which implied the distinction of protein conformation between p14^{ARF} and p19^{ARF}.

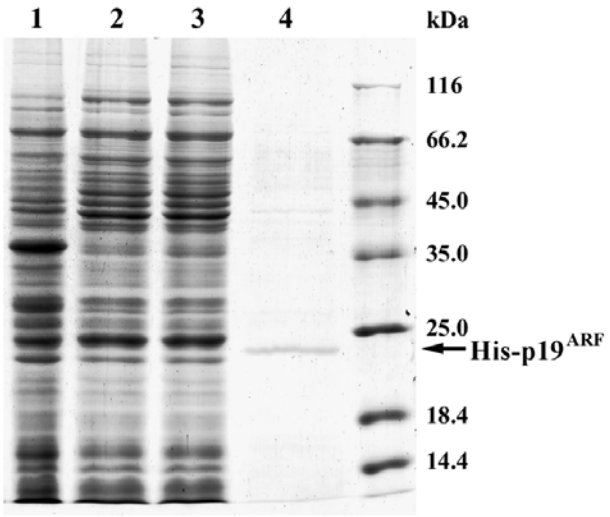

Fig. 1. SDS-PAGE analysis of expression and purification of 10His-p19^{ARF} from *E. coli*. Lanes: 1, whole cell extract, without IPTG induction; 2, whole soluble cell lysate, with IPTG induction; 3, flow-through fraction; 4, eluted 10His-p19^{ARF}

Immunoblot detection of 10His-p19^{ARF}: The Western blot result for the purified product was shown in Fig. 2. Compared with the 22 kDa eluted product detected by SDS-PAGE, the immunoblot emerged on the film confirmed clearly that present purified protein was His tagged p19^{ARF}.

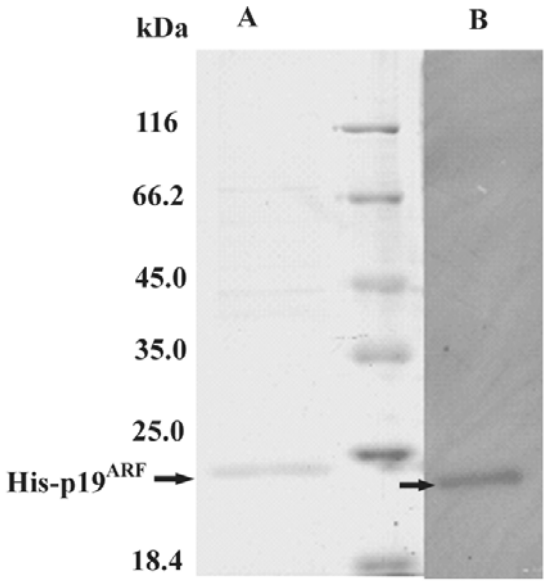

Fig. 2. Analysis of immunoblot detection. A, 12% SDS-PAGE for the eluted 10His-p19^{ARF} controlled by the molecular-mass marker protein; B, Western blot of this eluted 10His-p19^{ARF} emerged on the film

Interaction of 10His-p19^{ARF}ARF with TAp63γ: Pull-down assay was carried out to test the interaction of 10His-p19^{ARF} with TAp63γ. After extensive washing by buffer C to remove non-specifically bound protein, the materials on the glutathione-Sepharose were subjected to SDS-PAGE as shown in Fig. 3. 10His-p19^{ARF} showed interaction with immobilized GST-TAp63γ (Lane 2), while the beads immobilized GST did not pull down 10His-p19^{ARF} (Lane 3 and Lane 4).

This result demonstrated that the recombinant 10His-p19^{ARF} could inter-act with TAp63γ *in vitro*, suggesting that p19^{ARF} was capable of being expressed in a functional form in bacteria. Besides, as TAp63γ is a member of p53 tumor suppressor family and it is also a development regulator, the interaction between 10His-p19^{ARF} and TAp63γ indicated a concept that ARF might differentially regulate the expression of p53-target genes through the complex network of p53-like proteins, as a tumor suppressor or a development regulator.

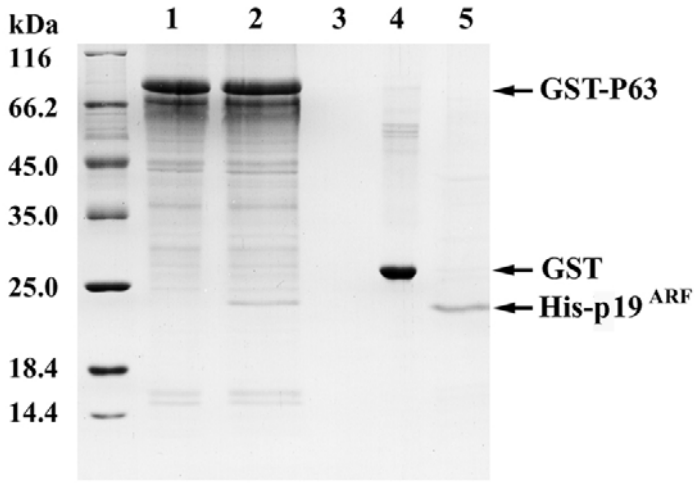

Fig. 3. GST-fusion protein pull-down assay. Lanes: **1**, the sample of beads immobilized GST-TAp63γ protein; **2**, pull-down of 10His-p19^{ARF} with beads immobilized GST-TAp63γ; **3**, glutathione-Sepharose beads which served as a negative control of pull-down assay; **4**, beads immobilized protein GST which served as a negative control of pull-down assay; **5**, the sample of eluted 10His-p19^{ARF}

Fluorescence analysis of 10His-p19^{ARF}: Fluorescence spectrum was used to investigate conformation of 10His-p19^{ARF} in solution. As shown in Fig. 4A, when the 10His-p19^{ARF} solution was excited at 280 nm, tyrosine fluorescence was not seen in the presence of tryptophan cause of the energy transfer. The characteristic emission apex at excitation wavelength of 295 nm was observed to be at 327 nm, which indicated that the Trp residues are located in a hydrophobic environment[23]. The C-terminal region (amino acids 130-169) which contains all Trp residues of p19^{ARF}, was involved in p53-independent apoptosis[21]. The hydrophobic feature of the environment of the three Trp residues suggested that the functional C-terminal region was hydrophobic.

The relative change of fluorescence emission maximum was plotted as a function of temperature in Fig. 4B. The data indicated that p19^{ARF} was relative stable in the range 20-50 °C. The intensity of fluorescence emission decreased with the temperature increasing from 60 to 80 °C. It was assumed that the thermal denaturation of 10His-p19^{ARF} involved a two-state transition, since no intermediate state was observed.

In Fig. 4C, fluorescence intensity was plotted as a function of pH and it was clear that the fluorescence intensity did not change significantly between pH 4 and pH 8. Fluorescence intensity decreased largely at pH 9. This result suggested that p19^{ARF} could endure a relative wide pH range.

The fluorescence emission intensity of 10His-p19^{ARF} decreased with the increase of β-mercaptoethanol (Fig. 4D). p19^{ARF} contained four Cys residues at positions 38, 81, 119 and 122. It was known that Cys residues are involved in the stabilization of the multimeric forms[24] of p14^{ARF} which gives the effect of β-mercaptoethanol on the fluorescence emission of p19^{ARF} in solution, it was probable that β-mercaptoethanol disrupted the structural integrity of p19^{ARF} by breaking the disulfide bond, which implicated that p19^{ARF} may have disulfide bond-dependent functional forms as p14^{ARF} did.

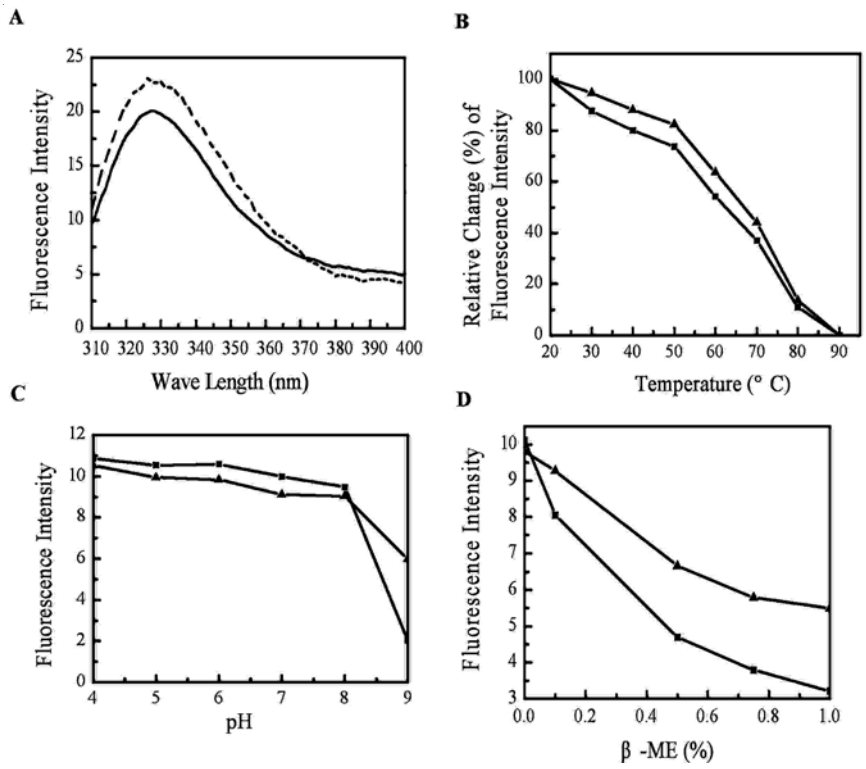

Fig. 4. Fluorescence spectra and intensity trends of 10His-p19^{ARF} in different microenvironments. **A**, Intrinsic fluorescence emission spectra carried out at 25 °C with 280 and 295 nm excitation wavelength. ------ the 10His-p19^{ARF} solution was excited at 280 nm; —— the 10His-p19^{ARF} solution was excited at 295 nm. **B**, Thermal denaturation curves of 10His-p19^{ARF} measured in terms of relative change of fluorescence intensity. 10His-p19^{ARF} was incubated for 0.5 h at different temperatures ranging from 20 to 90 °C. The relative change (%) of fluorescence intensity at 327 nm is given by $(\Delta I/\Delta I_{max}) \times 100$, where ΔI is the change in intensity from that in the native state and ΔI_{max} is the intensity change between the native and the denatured state at 90 °C. **C**, pH stability of 10His-p19^{ARF}. 10His-p19^{ARF} was incubated for 1 h in solutions at different pH, ranging from pH 4-pH 10. **D**, disulfide bond dependent stability of 10His-p19^{ARF}. 10His-p19^{ARF} was incubated for 4 h in solutions with different concentrations of β-mercaptoethanol. In Fig. 4 **B**, **C** and **D**, ■ Solutions were excited at 280 nm; ▲ Solutions were excited at 295 nm

ACKNOWLEDGEMENTS

This work was financially supported by the Ministry of Education of China for Excellent Youth Teacher Foundation (NCET-04-0861) and Sichuan University Research Grant 985.

REFERENCES

1. D.E. Quelle, F. Zindy, R.A. Ashmun and C.J. Sherr, *Cell*, **83**, 993 (1995).
2. T. Kamijo, F. Zindy, M.F. Roussel, D.E. Quelle, J.R. Downing, R.A. Ashmun, G. Grosveld and C.J. Sherr, *Cell*, **91**, 649 (1997).
3. C. Korgaonkar, J. Hagen, V. Tompkins, A.A. Frazier, C. Allamargot, F.W. Quelle and D.E. Quelle, *Mol. Cell Biol.*, **25**, 1258 (2005).
4. D. Chen, N. Kon, M. Li, W. Zhang, J. Qin and W. Gu, *Cell*, **121**, 1071 (2005).
5. Q. Zhong, W. Gao, F. Du and X. Wang, *Cell*, **121**, 1085 (2005).
6. N.E. Sharpless, *Mutat. Res.*, **576**, 22 (2005).
7. K. Tago, S. Chiocca and C.J. Sherr, *Proc. Natl. Acad. Sci. (USA)*, **102**, 7689 (2005).
8. S. Paliwal, S. Pande, R.C Kovi, N.E. Sharpless, N. Bardeesy and S.R. Grossman, *Mol. Cell Biol.*, **26**, 2360 (2006).
9. A. Tannapfel, C. Busse, F. Geißler, H. Witzigmann, J. Hauss and C. Wittekind, *Mol. Pathol.*, **55**, 379 (2002).
10. M. Wilda, J. Bruch, L. Harder, D. Rawer, A. Reiter, A. Borkhardt and W. Woessmann, *Leukemia*, **18**, 584 (2004).
11. N. Bardeesy, A.J. Aguirre, G.C. Chu, K.H. Cheng, L.V. Lopez, A.F. Hezel, B. Feng, C. Brennan, R. Weissleder, U. Mahmood, D. Hanahan, MN.S. Redston, L. Chin and R.A. Depinho, *Proc. Natl. Acad. Sci. (USA)*, **103**, 5947 (2006).
12. B. Eymin, C. Leduc, J.L. Coll, E. Brambilla and S. Gazzeri, *Oncogene*, **22**, 1822 (2003).
13. Y. Huang, T. Tyler, N. Saadatmandi, C. Lee, P. Borgstorm and R.A. Gjerset, *Cancer Res.*, **63**, 3646 (2003).
14. J.H. Berger and N. Bardeesy, *Curr. Mol. Med.*, **7**, 63 (2007).
15. V.H. Bokhoven and H.G. Brunner, *Am. J. Hum. Genet. A.*, **71**, 1 (2002).
16. M.I. Kostera and D.R. Roop, *J. Dermatol. Sci.*, **34**, 3 (2004).
17. T. Rinne, H.G. Brunner and V.H. Bokhoven, *Cell Cycle*, **6**, 262 (2007).
18. N.E. Sharpless, *Exp. Gerontol.*, **39**, 1751 (2004).
19. R. Wadhwa, T. Sugihara, M.K. Hasan, K. Tairo, R.R. Reddel and S.C. Kaul, *J. Biol. Chem.*, **277**, 36665 (2002).
20. S.J. Gallagher, R.F. Kefford and H. Rizos, *Int. J. Biochem. Cell Bio.*, **38**, 1637 (2006).
21. M. Matsuoka, M. Kurita, H. Sudo, K. Mizumoto, I. Nishimoto and E. Ogata, *Biochem. Biophys. Res. Commun.*, **301**, 1000 (2003).
22. A.E. Elaine, Current Protocols in Molecular Biology, Wiley, New York, p. 2958 (1996).
23. J.R. Lakowicz, Principles of Fluorescence Spectroscopy, Plenum Press, New York, p. 341 (1983).
24. S. Menéndez, Z. Khan, D.W. Coomber, D.P. Lane, M. Higgins, M.M. Koufali and S. Lain, *J. Biol. Chem.*, **278**, 18720 (2003).

(*Received*: 12 December 2007; *Accepted*: 20 August 2008) AJC-6768